Mirzaghavami *et al. Cancer Nanotechnology* (2022) 13:12
https://doi.org/10.1186/s12645-022-00120-3

Cancer Nanotechnology

RESEARCH Open Access

Folic acid-conjugated magnetic triblock copolymer nanoparticles for dual targeted delivery of 5-fluorouracil to colon cancer cells

Parvin Sadat Mirzaghavami[2], Samideh Khoei[1,2*], Sepideh Khoee[3] and Sakine Shirvalilou[1]

*Correspondence:
khoei.s@iums.ac.ir;
skhoei@gmail.com

[1] Finetech in Medicine Research Center, Iran University of Medical Sciences, P.O. Box: 1449614525, Tehran, Iran
Full list of author information is available at the end of the article

Abstract

Background: In the current study, folic acid-conjugated PEG-PCL-PEG triblock copolymer were synthesized and loaded with 5-fluorouracil and magnetite nanoparticles (5-FU-SPION-PEG-PCL-PEG-FA) for targeted delivery of drug to HT29 human colon cancer cells and CT26 mouse colon cancer model. The nanoparticles were synthesized and characterized by nuclear magnetic resonance spectroscopy (NMR) and transmission electron microscopy (TEM). The cellular uptake of nanoparticles was assessed in vitro (on HUVEC and HT29) and in vivo (on CT26 colon tumor tissues). The cytotoxic effect of nanoparticles was assessed on human colon cell lines (HT29, Caco-2, HTC116, and SW480) and normal HUVEC cells. In addition, antitumor effects of nanoparticles were investigated based on tumor volume, survival time and protein expression of Bax and Bcl-2 on CT26 tumor-bearing BALB/c mice.

Results: Characterization of nanoparticles showed 5-FU-SPION-PEG-PCL-PEG-FA (5-FU-NPs-FA) nanoparticles had spherical shape with hydrodynamic diameter of 85 nm. The drug-release profile exhibited sustained pH-responsive release with cumulative release reaching approximately 23% after 24 h. Cellular uptake studies revealed that HT29 cancer cells absorb higher amount of 5-FU-NPs-FA as compared to HUVEC normal cells ($P < 0.05$). In addition, 5-FU-NPs-FA was found to be more antitumor efficient in comparison to free 5-FU based on Bax/Bcl2 ratio, survival rate of tumoral mouse and inhibitory tumor volume ($P < 0.05$).

Conclusions: The results suggested that 5-FU-NPs-FA could be considered as promising sustained drug delivery platform for in vitro and in vivo conditions, which may provide selective treatment of tumor cancer cells.

Graphical Abstarct:

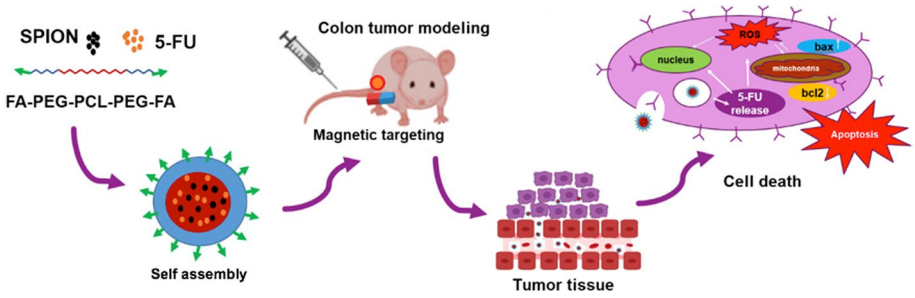

Keywords: Targeted drug delivery, Magnetite nanoparticles, Folic acid, Colon cancer, 5-Fluorouracil

Background

Colorectal cancer is among the three most prevalent cancers in both men and women with high rate of mortality (Siegel et al. 2017). 5-Fluorouracil (5-FU) is currently known as the first-line chemotherapeutic drug for treatment of colorectal cancer, which interferes with DNA and RNA synthesis through inhibition of thymidylate synthesis. However, severe side effects and a low response rate (approximately 15%) have been reported for this drug. The main reasons for its low efficiency include short half-life in plasma due to catabolization into inactive metabolites by dihydropyrimidine dehydrogenase (DPD), wide systemic body distribution and development of multidrug resistance (Longley et al. 2003; Mohammadi Gazestani et al. 2018). Developing nanotechnology-based drug delivery system has been suggested because of its ability to encapsulate and release drug in a controlled manner in specific sites. Accordingly, these systems are able to preserve drug from degradation enzymes that results in increased residence time of drug. Amphiphilic copolymers which consist of hydrophobic and hydrophilic parts are considered to be an efficient drug delivery system because of their ability to assemble into a micellar form with a hydrophobic core for encapsulating drug and a hydrophilic shell for increasing blood circulation time (Bodratti and Alexandridis 2018; Shirvalilou et al. 2020). Poly-ε-caprolactone (PCL) is hydrophobic polyester approved by FDA. Hydrolysis of PCL through esterase cleavage results in complete conversion to 6-hydroxycaproic acid, which is considered as natural metabolite in the body (Ferrari et al. 2013; Almeida et al. 2019). This hydrolytic degradation is a very slow process due to its high hydrophobicity and crystalline nature. PCL copolymerization using hydrophilic polymers like polyethylene glycol (PEG) can alter polymer crystallinity, permeability, solubility and thereby results in faster degradation rate depending on the utilized ratios. Accordingly, copolymer compounds consisting of PCL and PEG have attracted attention in the field of drug delivery research (Nguyen and Nguyen 2010; Wang et al. 2012; Wang et al. 2016; Wang et al. 2017).

Nanoparticles preferentially accumulate in the tumor through enhanced permeability and retention (EPR) (Stylianopoulos 2013). Furthermore, conjugating nanoparticles with specific ligands whose receptors are more expressed on cancer cells has been known as a promising approach for targeted delivery of drugs (Kumari and Kondapi 2017). Folic acid (FA), a hydrophilic vitamin with a low molecular weight has been considered as one

of these targeting ligand, as it is well known that folate receptors are overexpressed on the membrane of most of cancer cell lines (Song et al. 2012).

Incorporation of superparamagnetic iron oxide nanoparticles (SPION) into nanocarriers has been demonstrated to provide feasibility of detection and tracing through different technique such as Prussian blue staining, atomic absorption spectroscopy (AAS), inductively coupled plasma optical emission spectrometry (ICP-OES) and T_2-weighted magnetic resonance imaging (T_2W-MRI) (Asadi et al. 2018; Khoei 2021; Oghabian et al. 2011).

This study was conducted with the aim of taking more advantages of a PEG/PCL-based nano-micelle as a 5-FU delivery system through synthesizing a triblock copolymer conjugated with folic acid ligand. Thus, the SPION incorporated FA-PEG-PCL-PEG as a 5-FU carrier was synthesized and characterized using nuclear magnetic resonance spectroscopy and transmission electron microscope (TEM). The increased inhibitory effect of this approach in comparison to free drug of 5-FU was assessed against various colon cancer cell lines (including HCT116, SW480, HT29 and Caco-2) and human umbilical vein endothelial cells (HUVEC) using MTT cell viability assay. Afterward, the HT29 as the most 5-FU resistant colon cancer cell line was chosen for further experiments. To investigate the role of folic acid as a targeting ligand, cellular uptake of nanoparticles was evaluated in two different cell lines (HT29 and HUVEC) and colon tumor tissues.

Colon tumor model in BALB/c mice developed through implanting CT26 cancer cells into the mice leg. Additionally, the injected nanoparticles were conducted to the tumor site via exposing magnetic field owing to presence of SPION in their structure. Then, the cytotoxic effects of synthesized nanoparticles were investigated on colon tumor-bearing BALB/c mice based on tumor volume, survival time and expression of apoptosis related proteins (Bax and Bcl-2).

Results

Nuclear magnetic resonance analysis

^{1}H NMR spectra of synthesized polymers were obtained and shown in Fig. 1. The characteristic peaks of synthesized PCL were observed at about 4.1 (b), 1.6 (c) 1.4(d) and 2.3 ppm (e). Moreover, appearance of the three branched peaks at 4.2 ppm was attributed to methylene and ethylene glycol groups (Fig. 1A). As can be seen in spectrum B of this figure, a new peak appeared at 3 ppm as PCL was functionalized by adipoyl chloride which is attributed to methylene hydrogen in the vicinity of acyl group or carboxylic acid. Presence of intensified peak at 3.6 ppm was related to methylene groups of polyethylene glycol in the spectrum of PEG-PCL-PEG (spectrum C). Functionalization of triblock copolymer by folic acid was confirmed by appearance of peaks at 4.4, 6.5 and 7.5 ppm (Fig. 1D).

Size, zeta potential, morphology and in vitro release of nanoparticles

TEM analysis of drug-loaded NPs-FA confirmed that nanoparticles had a spherical shape with average particle size of about 50 nm (Fig. 2A). A schematic illustration of the NPs-FA structure is shown in Fig. 2B. Also, the hydrodynamic size of drug-free nanoparticles and drug-loaded nanoparticles was measured using DLS and found to have mean diameter 37.2 nm and 85 nm, respectively (Fig. 2C). TEM size of NPs-FA was smaller

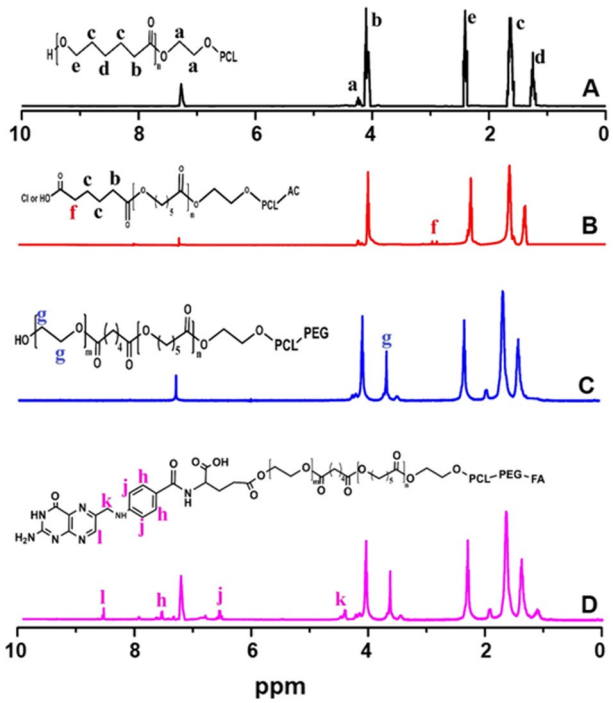

Fig. 1. ^{1}H NMR spectra of synthesized polymers: on **A** poly(ε-caprolactone) (PCL), **B** adipoyl chloride-functionalized PCL, **C** PEG-PCL-PEG, and **D** folic acid-functionalized PEG-PCL-PEG

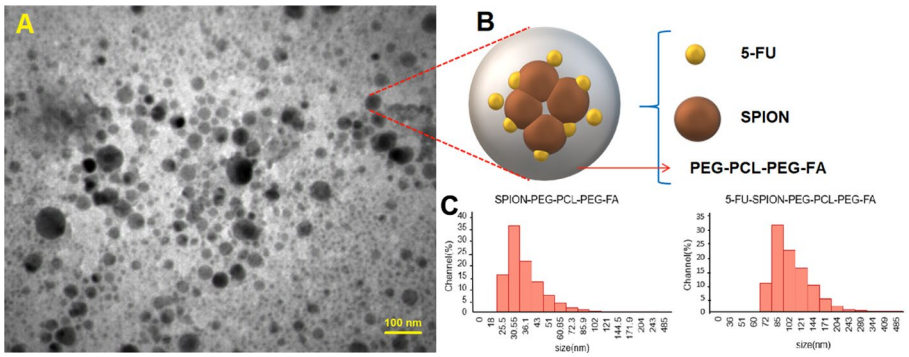

Fig. 2 Characterization of nanoparticles: **A** TEM image of 5-FU-SPION-PEG-PCL-PEG-FA, **B** schematic representation of 5-FU-SPION-PEG-PCL-PEG-FA, **C** size distribution measurements using DLS

than the hydrodynamic size measured by DLS which may be attributed to the attachment of H_2O molecules on the NPs during DLS analysis. As reported in our previous study (Mirzaghavami et al. 2021), drug-loading capacity (DLC) and encapsulation efficiency (EE) were calculated to be 5% and 56.5%, respectively. The in vitro cumulative release profiles of 5-FU from NPs-FA at 37 °C and different pH = 5.6, 6.8 and 7.4 are shown in Fig. 3. As illustrated, the more acidic the environment, the greater the release of the drug. As the tumor microenvironment is more acidic than normal tissue (Piasentin et al. 2020) the pH-responsive behavior of NPs may provide a suitable drug delivery system for controlled release of 5-FU. On the other hand, a biphasic release pattern consisting of an initial burst release, followed by a sustained drug release was observed.

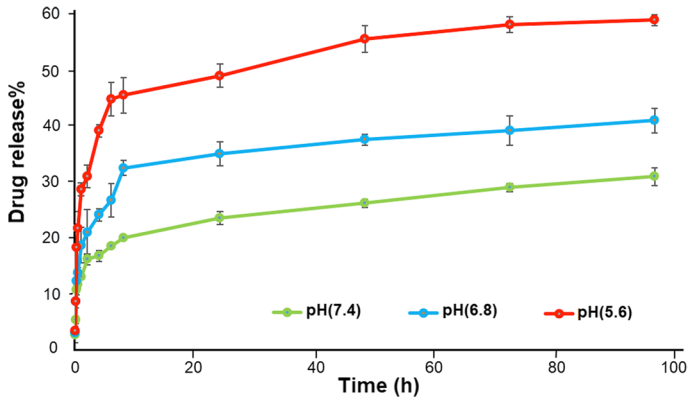

Fig. 3 In vitro 5-FU release in PBS at different pH (pH = 5.6, 6.8 and 7.4) at 37 °C

In the initial phase, 20.05 ± 0.33% of drug was released within 8 h. At later times, the rate of release tended to decrease such that After 48 h, the cumulative release reached 26.25 ± 0.78%. A continuous release was also observed for 15 days and ultimately, a cumulative release of 77.23 ± 3.96% was attained.

MTT assay

To investigate the cytotoxic effects of 5-FU and synthesized NPs-FA based on MTT assay, various concentrations of 5-FU and equivalent concentration of nanoparticles in the form of drug-free and drug-loaded were used to treat different cell lines. In this study, HT29, Caco-2, SW480 and HCT116 were chosen as colon cancer cell lines. Additionally, HUVEC cells were included as a representative of normal cell lines. As shown in Fig. 4A–E, the cytotoxicity of 5-FU, 5-FU-loaded and drug-free nanoparticles against these cell lines were concentration dependent. The half-maximal inhibitory concentration (IC50) value of 5-FU, 5-FU-loaded and drug-free nanoparticles against aforementioned cell lines were calculated based on MTT viability curves and illustrated in Table 1. According to this result, the IC50 values of 5-FU-loaded nanoparticles for colon cancer cell lines were greatly lower than that of free 5-FU, whereas the difference of IC50 between free and encapsulated 5-FU was much smaller in the case of HUVEC normal cells (5.2 ± 0.79 μM vs 3.86 ± 0.11 μM).

These results demonstrated that at equivalent concentration of 5-FU, treatment with 5-FU-loaded nanoparticle leads to significantly lower viability in colon cancer cell lines compared with free 5-FU. This indicates reduced dose of drug would be required to inhibit cancer cells which in turn leads to decrease in side effects and normal tissue damage. This finding can be justified due to presence of folic acid ligand that facilitates entrance of nanoparticles into folate receptor-positive cancer cells through receptor-mediated endocytosis. Overexpression of folate receptor on most of cancer cells such as colorectal cancer cells has been confirmed and exploited in numerous researches (Didion and Henne 2020). In the following, HT29 cells were selected because of their highest resistance to 5-FU among colon cancer cells for further investigations. To further compare the inhibitory effect of 5-FU with

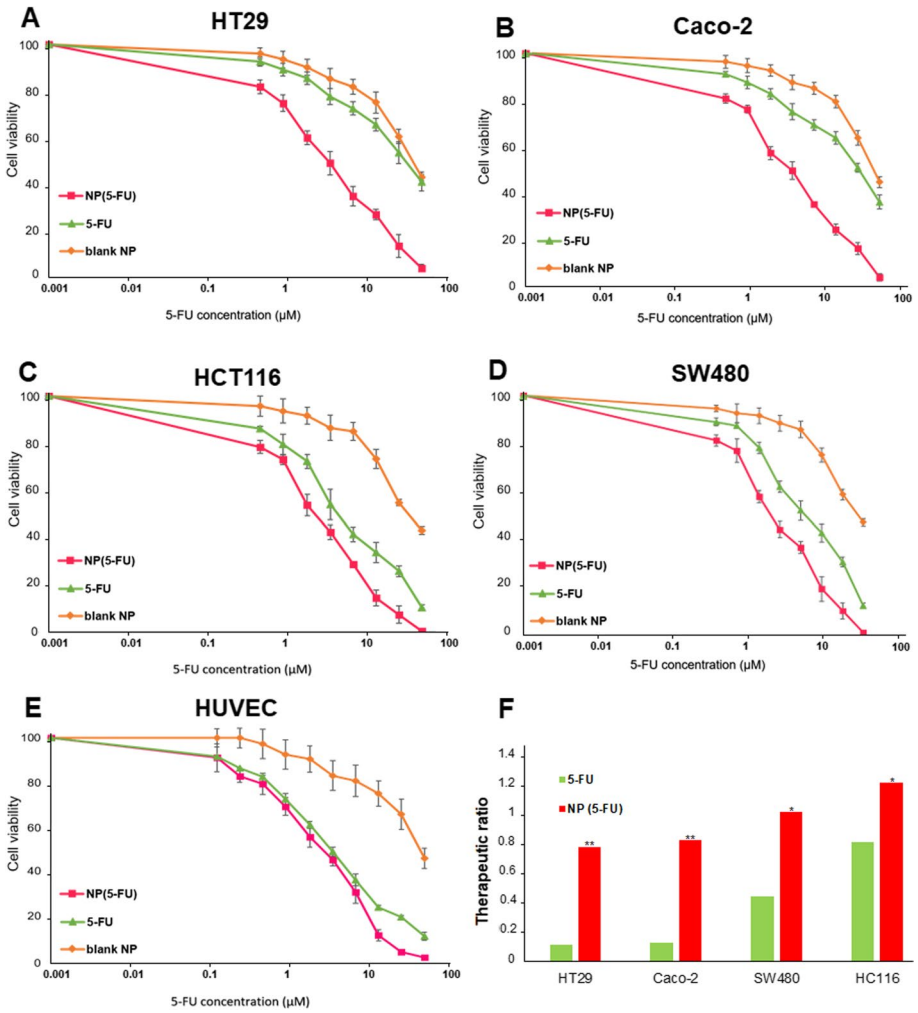

Fig. 4 In vitro cell viability assessment using MTT assay after 48 h incubation of **A** HT29, **B** Caco-2, **C** HCT116, **D** SW480 and **E** HUVEC cells with drug-free NPs, 5-FU, and 5-FU-loaded NPs; **F** calculated therapeutic ratios for colon cancer cell lines

Table 1 Calculated IC50 of 5-FU and 5-FU-loaded NPs against different cell lines based on MTT cell viability curves

Treatment	HT29	Caco-2	SW480	HC116	HUVEC
5-FU	46.1 ± 4.7	41.9 ± 1.5	12.0 ± 2.2	6.5 ± 0.3	5.2 ± 0.7
SPION-PEG-PCL-PEG-FA	62.6 ± 3.8	69.1 ± 2.3	69.4 ± 3.8	55.4 ± 1.4	71.4 ± 1.8
5-FU-SPION-PEG-PCL-PEG-FA	5.1 ± 0.88	4.8 ± 0.7	3.9 ± 0.4	3.2 ± 0.2	3.8 ± 0.1
IC50 (5-FU)/ IC50 (5-FU-SPION-PEG-PCL-PEG-FA)	9.04	8.72	3.07	2.03	1.37

5-FU-loaded nanoparticle, a therapeutic index which was defined as the ratio of IC50 of normal cell to IC50 of cancer cell as illustrated in Fig. 4F.

IC10 concentration of 5-FU was calculated according to its cell viability curve against HT29 cells (2.25 μM). The equivalent concentration of NPs containing same

amount of 5-FU was calculated using DLC% and percentage of cumulative release at 48 h (21.9 μg/mL). These concentrations were chosen as treatment dose to be employed for further experiments.

Cellular uptake of NPs-FA in vitro and in vivo

The uptake of nanoparticles in HUVEC and HT29 cell lines after 48 h with 21.9 μg/ml of NPs was confirmed by the Prussian blue staining (Fig. 5A). The quantitative cellular uptake was also assessed using ICP-OES method by measuring iron concentration. Based on this experiment, the average iron content was 2.96 ± 0.27 and 12.65 ± 1.2 pg/cell for HUVEC and HT29, respectively. Higher adsorption of the NPs-FA to HT29 cells in comparison to HUVEC cells indicates efficacy of folic acid as a targeting ligand in achieving receptor-mediated endocytosis. The in vivo study of uptake of nanoparticles into tumor tissues with NPs and NPs-FA is shown in Fig. 5B. As shown, nanoparticles with conjugated folic acid have higher uptake in tumor tissue than nanoparticles without ligand.

In vivo antitumor effects of nanoparticles

Tumor volume and survival time of tumor-bearing mice

The antitumor effect of free 5-FU, NPs-FA with/without drug loaded was evaluated in mice colon cancer model developed through implanting CT26 cancer cells into mice leg by tumor volume and survival rate. 20 days after starting treatment with saline, free 5-FU, NPs-FA and 5-FU loaded NPs-FA, the tumor volume reached 3898, 1495, 3217, and 613 mm^3 (Fig. 6A). Free 5-FU significantly inhibited tumor growth ($P < 0.01$), however, over time, the tumor volume increased ($P > 0.05$). The 5-FU loaded NPs-FA group, showed a significant inhibition of tumor volume on the day 30 ($P < 0.05$), whereas, as shown in the survival curve results (Fig. 6B), the mice in this group survived until the 50th day. The median survival time of mice in the four treatment groups was as follows: saline (22) < NPs-FA (27) < 5-FU (33) < 5-FU loaded NPs-FA (48 day). Figure 6B shows the Kaplan–Meier plot. Kaplan–Meier estimate is one of the best options to be used to measure the fraction of subjects living for a certain amount of time after treatment. The results demonstrated that the FA ligand increased the therapeutic efficiency of drug

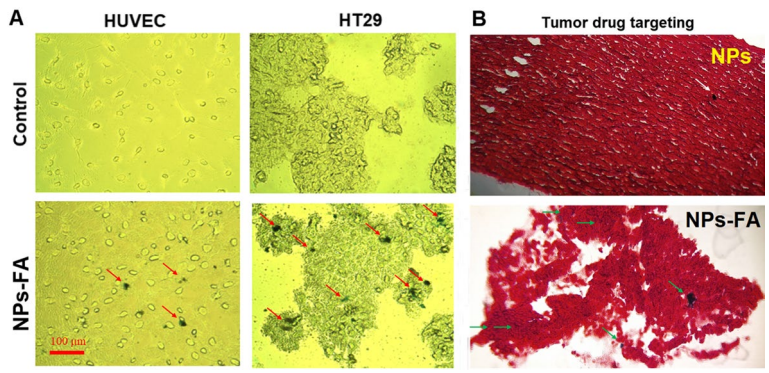

Fig. 5 **A** Uptake of NPs-FA by HUVEC and HT29 cells after 48 h incubation. **B** Uptake of NPs and NPs-FA by colon tumor tissues

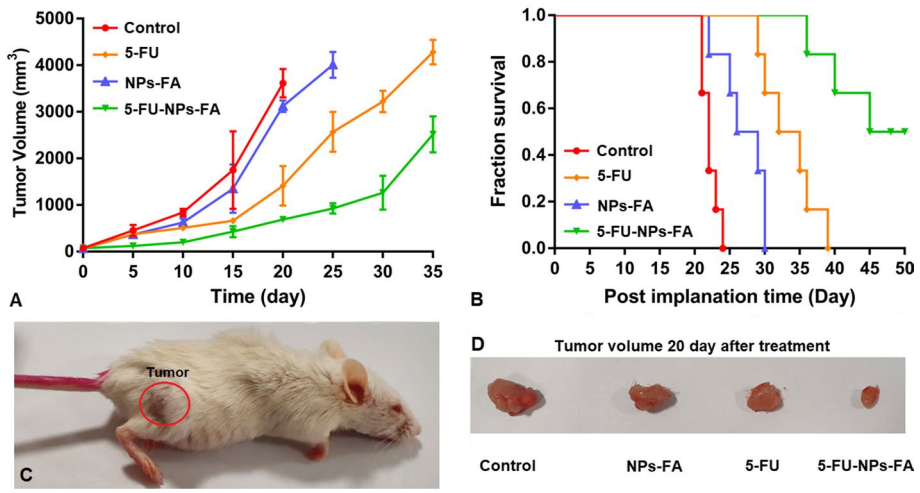

Fig. 6 Antitumor efficacy of free 5-FU, NPs-FA and 5-FU-loaded NPs-FA in the presence magnetic field were determined in the CT26 colorectal tumor model. **A** Tumor volume in different treatment groups, **B** Kaplan – Meier plot, **C** photographs of colon tumor-bearing mice, **D** tumor volume in control and treated groups (mean ± SD, $n = 6$)

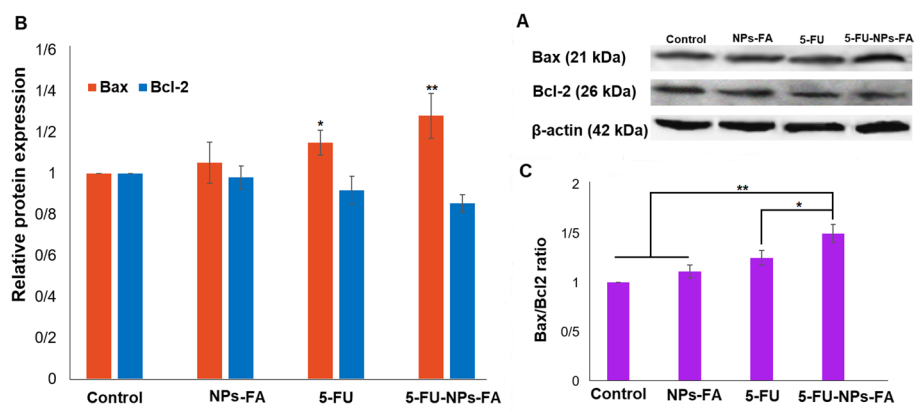

Fig. 7 **A** Protein expression detected by Western blot. **B** effects of drug-free NPs-FA, 5-FU, and 5-FU-loaded NPs-FA on relative protein expression of Bax and Bcl-2; **C** Bax/Bcl-2 ratio in tumoral mice after 48 h of treatments. *$P < 0.05$; **$P < 0.01$

and NPs ($P < 0.01$). Figure 6C shows tumor-bearing mice. The tumor volume shown in Fig. 6D confirms that 5-FU-loaded NPs-FA, 20 days after treatment exhibits the strongest antitumor effect on colon cancer compared to other treatment groups relative to the control group ($P < 0.01$, Fig. 6A).

Protein expression study of Bax and Bcl2

The protein expression of Bax and Bcl-2 was investigated to compare the apoptotic effects of 5-FU, 5-FU loaded NPs-FA and drug-free NPs-FA (Fig. 7A). As depicted in Fig. 7B, implementation of these treatments at equivalent 5-FU concentration led to upregulation of Bax protein in 5-FU ($P < 0.05$) and 5-FU loaded NPs-FA groups ($P < 0.01$), while insignificant change in Bax protein was observed for drug-free NPs-FA. The

changes in level of Bcl-2 protein found to insignificant. The ratio of Bax/Bcl-2, which is known as regulator of apoptosis, was calculated for different treatments (Fig. 7C). Bax/Bcl2 ratio was remarkably higher in 5-FU and 5-FU-loaded NPs compared to control group ($P < 0.01$). It was also found that 5-FU-loaded NPs-FA results in further increase of Bax/Bcl2 ratio in comparison with 5-FU ($P < 0.01$). This finding emanates from increased concentration of intracellular 5-FU provided by anchoring of folic acid-conjugated nanoparticles to folate receptors on tumor cells that facilitate endocytosis process. Western blotting analysis showed that changes in protein expression of Bax and Bcl2 were in agreement with the result of gene expression reported in our previous study (Fig. 7) (Mirzaghavami et al. 2021).

Discussion

Although 5-FU is known as the mainstream in chemotherapy of broad range of cancers including breast and colorectal cancers, its short half-life in plasma, as well as wide systemic distribution, hinder it from reaching tumor sites. This drawback necessitates intermittent administration of high dose 5-FU which leads more severe side effects such as cardiotoxicity, vomiting, diarrhea, and severe anemia (Mattos et al. 2016; Eynali et al. 2017). This issue can be addressed by incorporating 5-FU into polymeric nanoparticles through increasing blood circulation time and providing controlled drug release. In current study, a sustained release has been provided by incorporating drug into synthesized polymer which is due to presence of PCL in copolymer structure. Because PCL is highly hydrophobic, it resists water penetration that implies very slow rate of degradation. However, this behavior of PCL is modified by copolymerization with PEG that results in accelerating degradation to some extent that is required for a drug nanocarrier (Wang et al. 2001; Ashour et al. 2019). Furthermore, it has been demonstrated that hydrophobic/hydrophilic ratio has crucial role in stabilizing of formed micelle. It has been also reported the micelles formed by triblock copolymer are more advantageous over diblock formed micelles in terms of stability which is attributed to lower critical micelle concentration (CMC) of triblock copolymers (Lin et al. 2006). CMC is an important parameter that determines stability of micelle at diluted concentration. Having low CMC prevents from disintegration of micelle after diluting in blood stream. Hence, designing ultra-low CMC is considered as a topic in the field drug delivery researches (Lu et al. 2018). PCL-PEG-PCL is a type of PCL/PEG-based triblock which has been utilized as 5-FU carrier which has faster drug-release rate than that observed for our nano-formalism (Asadi et al. 2018). A comprehensive evaluation on PCL/PEG-based triblock, consisting PCL-PEG-PCL and PEG-PCL-PEG with different ratio of copolymerization, has demonstrated that CMC values of PEG-PCL-PEG type are about half of those measured for its identical PCL-PEG-PCL which indicates higher stability of PEG-PCL-PEG type (Zamani and Khoee 2012). Thus, based on these evidences, the molecular weights of 2000 and 6000 g/mol were considered for PEG and PCL, respectively, to synthesize PEG-PCL-PEG triblock. Amphiphilic copolymers possess ability to assemble into a micellar form with a hydrophobic core for encapsulating drug and a hydrophilic shell for increasing stability and blood circulation time. Accordingly, PCL core of micelles are encapsulation site for 5-FU. Furthermore, it is also possible that 5-FU loading onto PCL NPs benefit from electrostatic attractive forces that may exist between the positively charged drug

molecules (generated by protonation of the NH group of the 5-FU chemical structure), and the negatively charged polymeric NPs. Additionally, prolonged drug release indicates that drug has been located in the core region of nanoparticles. To take advantage of active targeting, folic acid was conjugated to the triblock copolymer. As folic acid acts as a coenzyme in different cellular process such as DNA synthesis, repair and cell division, folate receptors are mainly overexpressed on the surface of most of cancer cells owing to their higher metabolism (Zhao et al. 2008). To examine whether the nanoparticle is actively targeted, cell viability using MTT assay was achieved on colon cancer cell lines (as folate receptor positive) and HUVEC cells (as folate receptor negative). In the case of treatment with 5-FU in the form of free drug, we observed HUVEC cells (the normal cell line) underwent severe cytotoxicity compared to HT29 regarding to their obtained IC50. This may attributed to high expression of multidrug resistance associated genes in cancer cells (Plasencia et al. 2006). Moreover, it was found that whereas IC50 of 5-FU-loaded NPs against colon cancer cells (HCT116, SW480, HT29 and Caco-2) was drastically reduced compared to that of 5-FU alone, a mild decrease was seen in that of HUVEC. This indicates higher percent of cancer cells inhibition for a given level of normal cell cytotoxicity can be achieved by means of treatment with 5-FU-loaded NPs which implies increased therapeutic index. This results is in accordance to what we expected due to folate receptor-mediated endocytosis which is dominant in HT29 cells (Wang et al. 2015; Handali et al. 2018) while HUVEC cells are known to express very low level of folate receptor (Qiu et al. 2018). The targeting role of folic acid has been confirmed by Wang et al. They have reported An IC50 of 5.69 mg/mL for 5-FU-loaded PLGA-1, 3-diaminopropane-folic acid nanoparticles against HT29 cells that is considerably lower than IC50 of 14.17 and 22.91 mg/mL for 5-FU loaded PLGA and 5-FU alone, respectively (Wang et al. 2015). San et al. found that cellular uptake of Fol-Cur-NPs was greater than Cur-NPs in folate receptor expressing Y79 cells, whereas no significant difference in cellular uptake of Fol-Cur-NPs and Cur-NPs was found in folate receptor non-expressing A549 cells. The IC50 of Fol-Nut-Cur-NPs for Y79 cells was found to be 35 and 8.6 times lower compared to free drugs and unconjugated drug-loaded NPs (Das and Sahoo 2012). Another study that could be mentioned in case of enhancing effect of folic acid conjugation was conducted by Akinyelu et al. (2019). They observed more significant cytotoxicity and apoptosis in MCF7 cells treated by 5-FU-loaded folate-tagged chitosan-gold nanoparticles. Additionally, the role of folic acid as a targeting ligand has also been confirmed by in vivo evaluation. Figure 5 shows that the presence of folic acid ligand causes more NPs to enter the tumor tissue, which can improve targeted drug delivery to the tumor.

Antitumor efficacy of 5-FU and 5-FU-loaded NPs was corroborated at utilized dose by different endpoints. This foundation could be ascribed to action of 5-FU. Further assessment indicated 5-FU loaded NPs possess more inhibitory efficiency than 5-FU on colon cancer (Mohammadi Gazestani et al. 2018). This claim was approved according to higher ratio of Bax/Bcl-2, increased survival time, and inhibition of tumor volume in mice treated with 5-FU loaded NPs-FA. This finding can be justified by considering their different cellular uptake pathways. It is well known that 5-FU as hydrophilic drug has a poor penetration into cell through diffusion and is highly prone to be washed out while NPs could internalize into cell via endocytosis (Handali et al. 2019; Sharma et al. 2017;

Esmaelbeygi et al. 2015). Endocytosis of NPs has been shown as an approach to bypass drug efflux pumps and subsequently reverse multidrug resistance (Zhou et al. 2019). In current study, folic acid conjugation was done to take advantage of a more efficient type of endocytosis which is mediated by ligand–receptor interaction. Afzali et al. also reported that when the nanoparticles were modified with folic acid, the distribution of nanoparticles in the glioma tumor was significantly higher than in healthy brain tissue (Afzalipour et al. 2019).

Another study that could be mentioned in case of enhancing effect of folic acid conjugation was conducted by Rajpootet et al. (2020). They observed more significant cytotoxicity and apoptosis in colorectal Balb/c mice treated by irinotecan-loaded folate-grafted solid lipid nanoparticles. Their results showed that FA-coupled nanoparticles distributed higher amount of drug as compared to uncoupled nanoparticles in the colon tumor after 48 h (Rajpoot and Jain 2020).

Conclusions

In the current study, folic acid-conjugated PEG-PCL-PEG triblock copolymer was synthesized and subsequently loaded with 5-FU and magnetite nanoparticle to constitute 5-FU-SPION-PEG-PCL-PEG-FA nanoparticles. This nanoparticle showed a sustained and pH-responsive drug release due to crystallinity of PCL and high hydrophobic/hydrophilic ratio. This characteristic feature would obviate the necessity of intermittent administration of 5-FU. This formalism was found to possess enhanced antitumor efficacy as compared to same concentration of free 5-FU as the result of receptor-mediated endocytosis. Therefore, it can be concluded that 5-FU-SPION-PEG-PCL-PEG-FA has the potential to be utilized as a targeted drug delivery system for selective treatment of colon cancer tumor with reduced dose of drug.

Methods

Synthesis of 5-FU-SPION-PEG-PCL-PEG-FA nanoparticles

We have previously reported the synthesis of 5-FU-SPION-PEG-PCL-PEG-FA nanoparticles by a modified W1/O1/W2 double emulsion solvent evaporation method (Mirzaghavami et al. 2021). These nanoparticles were synthesized in 5 steps in the following order (Fig. 8).

Step 1: synthesis of poly (ε-caprolactone) (PCL)

3 ml of ε-caprolactone (27 mmol) was dissolved in 5 ml of dimethylformamide (DMF) in a three-necked round-bottom flask. Then, 5 µl of ethylene glycol (1 mmol) was added under a nitrogen atmosphere. The reaction temperature was gradually increased to 80 °C followed by addition of stannous octoate [Sn $(Oct)_2$] and increasing temperature to 120 °C. After 24 h, the polymer was precipitated in water at 0 °C and then dried at 40 °C. In order to purify polymer, it was dissolved in DMF and precipitated in water. The product was obtained with 82% yield.

Step 2: synthesis of adipoyl chloride-functionalized PCL

1g of caprolactone (0.2 mmol) was dissolved in DMF and 146 µl (1 mmol) of adipoyl chloride and catalytic amount of triethylamine was added. The reaction was continued

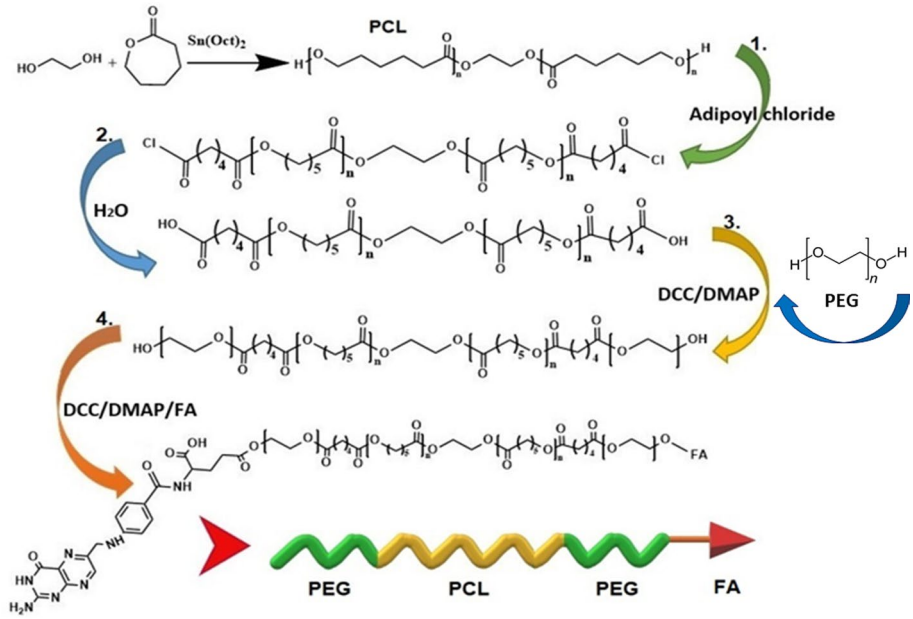

Fig. 8 Schematic representation of triblock copolymer synthesis steps

for 24 h at 80 °C. Then functionalized polymer was precipitated in water followed by drying in the vacuum oven at 40 °C. The purified product was obtained by dissolution of crude product in DMF and then precipitated in cold water.

Step 3: synthesis of PEG-PCL-PEG

1 g of functionalized PCL was dissolved in 10 mL of dimethyl sulfoxide (DMSO) and afterward 206 mg *N*,*N*′-dicyclohexylcarbodiimide (DCC) and 122 mg 4-dimethylaminopyridine (DMAP) was gradually added to solution. After 1 h, 2 g of PEG was added and stirred at room temperature for 24 h. PEG-PCL-PEG copolymer was precipitated in diethyl ether and then dried in vacuum oven at 40 °C. To have more purified product, dissolving in DMSO and precipitating in diethyl ether was repeated.

Step 4: synthesis of folic acid-functionalized PEG-PCL-PEG

220 mg of folic acid, 103 mg of DCC and 61 mg of DMAP were dissolved in 10 mL of DMSO and the reaction was continued for 4 h to activate acidic group of folic acid. Then 1 g of PEG-PCL-PEG copolymer was added and the reaction was continued overnight. After 24 h, the product was precipitated in diethyl ether and dried at 40 °C. Dissolving in DMSO and precipitating in diethyl ether was repeated to acquire more purified product (Fig. 8).

Step 5: synthesis of 5-FU-loaded magnetite/PEG-PCL-PEG-folic acid

Preparation of the 5-FU-loaded magnetite/PEG-PCL-PEG-folic nanoparticles was performed by using W1/O1/W2 double emulsion solvent evaporation method. For preparation of inner aqueous solution (W1), 10 mg of 5-FU drug was dissolved in 1.5 mL of distilled water containing 10 mg of Tween 60. 30 mg of magnetite nanoparticles was

dispersed in 7 mL of dichloromethane (DCM) to prepare an organic phase using an ultrasonic probe. Then 50 mg of the folic acid-conjugated polymer (PEG-PCL-PEG-FA) and 200 mg of Span 60 were added to the oil phase (O1). W2 aqueous solution was made of 100 mg tween 60 dissolved in 8 mL of distilled water and 8 mL of glycerin. The inner aqueous solution (W1) was emulsified in the organic phase (O1) by ultrasonication using the sonicator probe at an output of 50 W for 30 s in an ice-bath to obtain a W1/O1 emulsion. This primary emulsion was emulsified in second aqueous solution (W2) by ultrasonication for 30 s (50 W) in an ice-bath to obtain a W1/O1/W2 double emulsion. The resulting double emulsion was diluted in 30 mL aqueous solution composed of 15 mL distilled water and 15 mL glycerin under mechanical stirring for a period of 3 h at room temperature, and the DCM was removed by solvent evaporation. The obtained magnetic nanoparticles were cleaned by repeating procedure of collecting and re-suspending in distilled water for two times and then were collected with a magnet. Finally, the resulting nanoparticles were dried by freeze-drying and stored at 4 °C. Drug-free nanoparticles were prepared in the same way, except that the inner aqueous solution was prepared with 1.5 mL of distilled water and 10 mg of tween60, but without 5-FU drug.

Proton nuclear magnetic resonance analysis

In order to investigate synthesis procedure and characterize the structure of the synthesized products, the ^{1}H nuclear magnetic resonance (NMR) analysis was performed on poly (ε-caprolactone) (PCL), adipoyl chloride-functionalized PCL, PEG-PCL-PEG and folic acid-functionalized PEG-PCL-PEG using a Varian Inova, 500 MHz spectrometer. Deuterated chloroform ($CDCl_3$) was used as solvent of samples to acquire ^{1}H NMR spectra.

Characterization of size, zeta potential and morphology of nanoparticles

Dynamic light scattering (DLS) analysis was used to characterize the distribution of the hydrodynamic size of drug-free and 5-FU-loaded nanoparticles. The surface charge of nanoparticles was evaluated by Zeta sizer (Nanoflex, Germany).

The morphology of 5-FU-loaded nanoparticles was investigated using a transmission electron microscope (TEM, Zeiss LEO906, Germany). The samples were prepared on 400-mesh carbon-coated copper grid and imaged at accelerating voltage of 100 kV.

In vitro drug-release profiles

Investigation of in vitro release profile of 5-FU from NPs-FA was carried out based on equilibrium dialysis bag diffusion method at different pH (5.6, 6.8 and 7.4). First, 3 mg of 5-FU loaded NPs-FA was suspended in phosphate buffer saline (PBS) with different pH and transferred to a dialysis bag (MWCO 12,400 Da). The dialysis bag was fully immersed into a tube containing 10 mL PBS and stirred at the shaking speed of 100 rpm at 37 °C. At predetermined time points, 1.5 mL of media was sampled and replaced with an equal volume of PBS. The absorption of released 5-FU was measured using an UV-spectrophotometer at 265 nm.

Cell culture

The colon cancer cell lines (HCT116, SW480, HT29 and Caco-2) and HUVEC cells were purchased from Stem Cell Technology Research Center and, respectively, cultured in complete RPMI and DMEM/Ham's F-12 medium supplemented with 10% FBS, penicillin (100 U/mL) and streptomycin (100 mg/mL) under humidified incubator with 5% carbon dioxide at 37 °C.

Allograft mouse colon tumor models

The CT26 mouse colon cancer cells and BALB/c mice (20–30 g) were purchased from Pasteur Institute of Tehran, Iran. Mice were kept under the standard conditions in accordance with the Helsinki Declaration at the Animal Research Center of Iran University of Medical Sciences, Tehran, Iran. For colon tumor modeling, 2×10^6 of CT26 cells in 100 µL of RPMI medium were injected subcutaneously on the right leg of the mice.

MTT assay

The cellular cytotoxicity of 5-FU and synthesized nanoparticles was investigated using MTT assay. In brief, HUVEC and colon cancer cell lines (HCT116, SW480, HT29 and Caco-2) were cultured in a 96-well plate at a density of 7×10^3 cells per well. After 24 h, the cells were treated with varying concentrations of 5-FU ranging from 0.6 to 80 µM and equivalent concentrations of drug-free and drug-loaded NPs. After 48 h incubation, the cells were washed and treated with MTT (5 mg/mL). Plates were incubated at 37 °C in the dark. After 4 h, the medium containing MTT was removed, and 100 µL of dimethyl sulfoxide (DMSO) was added. The solution was incubated for 15 min to solubilize formazan crystals. The absorbance was measured at 570 nm using a microplate reader (BioTek, Winooski, VT). Finally, cell viability was determined based on Eq. (1):

$$\text{Cellviability}(\%) = \frac{\text{absorbance of treated cells}}{\text{absorbance of control cells}} \times 100. \quad (1)$$

To compare the cytotoxicity of 5-FU with 5-FU-loaded nanoparticle on the cell lines, the IC50 values of these agents was calculated regarding to cell viability curves and also a therapeutic index was defined as the ratio of IC50 of normal cell to IC50 of cancer cell.

According to MTT results, the most 5-FU-resistant cell line that necessitates using higher dose of drug, was selected for further assessments.

Cellular uptake of NPs-FA in vitro

Prussian blue staining

The cellular uptake of NPs-FA was visually investigated using the Prussian blue staining assay. The HT 29 and HUVEC cell lines were seeded in 6-well plates. After 24 h, both cell lines were incubated with amount of SPION-PEG-PCL-PEG-FA NPs which has capability of encapsulating IC10 of 5-FU against HT29 within 48 h. After treatment time, the cells were washed with PBS for three times, then fixed with

4% paraformaldehyde solution for 20 min followed by staining with the Prussian blue solution (2% potassium ferrocyanide and 2% hydrochloric acid with 1:1 ratio) for 30 min. Subsequently, cells were washed with PBS, and imaged using an optical microscope at the magnification of 400× (Olympus CK2; Olympus Optical Co., Tokyo, Japan).

Inductively coupled plasma optical emission spectrometry (ICP-OES)

In order to quantitatively evaluate the cellular uptake of NPs-FA, both cell lines were cultured in T-25 cell culture flasks at a density of 5×10^5 cells, treated in the same way as described before. After treatment, the cells were washed with PBS, trypsinized, collected and counted for quantification purposes. The cells were digested with 1 mL of concentrated HNO_3 at 140 °C for 2 h. The samples were diluted to 5 mL with deionized water and the concentration of iron was measured using an ICP-OES assay (VISTA-PRO, Varian, Australia). Finally, the average iron content per cell was calculated.

Cellular uptake of NPs and NPs-FA in vivo

The accumulation of NPs and NPs-FA in colon tumor tissues was assayed by Prussian blue staining. The mice were injected with 20 mg/kg NPs with/without drug (containing 1 mg/kg of free 5-FU) through the tail veins 14 days after tumor implantation. For magnetic drug targeting, the magnets with magnetic intensity of 1.3 T were placed on the mice colon tumor for 1 h. Tumoral mice were killed 1 h after the injection of nanoparticles with or without folic acid and magnetic targeting. For magnetic drug targeting, the magnets were placed on the mice colon tumor for 1 h. After, the tumor tissues were fixed in formalin solution (10%) for 48 h at 25 °C. The samples were dehydrated in different concentrations of ethanol, embedded in paraffin, cryosectioned, and stained with Prussian blue solution. The sections were incubated with a mixture of 10% potassium ferrocyanide and 20% hydrochloric acid for 20 min, then washed and stained with Nuclear Fast Red.

In vivo antitumor effects of nanoparticles

Colon tumor model was developed in BALB/c mice (20–30 g) by injecting 2 million CT26 cells. After 12 days, when the tumor size reached about 70 to 100 mm^3, the mice were divided into 4 groups of 9:

Group 1: normal saline (control),

Group 2: Free 5-FU solution,

Group 3: SPION-PEG-PCL-PEG-FA (NPs-FA) and magnet for 1 h,

Group 4: 5-FU-loaded NPs-FA and magnet for 1 h.

(Only mice in the treatment groups that received the nanoparticles were exposed to the magnetic field for one hour.) The mice were treated with 5-FU and NPs-FA with/without drug injections through the tail veins every other day (12, 14 and 16 days) of the experiment with 1 mg/kg of free 5-FU and 20 mg/kg of NPs-FA (containing 1 mg/kg of 5-FU). After the treatments, the tumor size was measured daily and the tumor volume was calculated by the following equation:

$$V = \left[\text{width}^2/2\right] \times \text{length}. \quad (2)$$

Furthermore, the 6 mice in each group were monitored for life span and analyzed by the Kaplan–Meier survival curves.

Western blotting analysis

Two days after treatment, protein level changes of Bax and Bcl-2 in colon tumor-bearing mice was assessed by Western blotting assay. Tumor tissues were homogenized and total protein extracted with RIPA lysis buffer (Santa Cruz Biotechnology, USA) and quantified using Bradford protein assay. The proteins separated through gel electrophoresis were transferred to nitrocellulose membrane. These membranes were incubated for 24 h at 4 °C in the solution containing the primary antibodies: Bax (1:500), Bcl-2 (1:1000) and β-actin (1:500). Subsequently the membranes were washed with mixture of Tris buffered saline and Tween 20 (TBST) and then incubated with a horse radish peroxidase conjugated-secondary antibody. Finally, the protein bands were visualized using enhanced chemiluminescence western Blotting Detection Reagent (ChemiDocXRS; Bio-Rad, South San Francisco, USA). The protein bands were quantified using ImageJ software and then normalized to intensity of β-actin.

Statistical analysis

The results of all experiments were expressed as mean ± standard deviation and analyzed using one-way analysis of variance (ANOVA) followed by Tukey's test using Graphpad prism 6. A *P*-value of 0.05 or lower was considered to be statistically significant.

Abbreviations

5-FU: 5-Fluorouracil; AAS: Atomic absorption spectroscopy; ANOVA: Analysis of variance; CMC: Critical micelle concentration; DCC: *N*,*N*′-Dicyclohexylcarbodiimide; DCF: 2′,7′-Dichlorofluorescein; DCFH-DA: 2′,7′-Dichlorofluorescein diacetate; DCM: Dichloromethane; DLC: Drug loading capacity; DLS: Dynamic light scattering; DMAP: 4-Dimethylaminopyridine; DMF: Dimethylformamide; DMSO: Dimethyl sulfoxide; DPD: Dihydropyrimidine dehydrogenase; EE: Encapsulation efficiency; EPR: Enhanced and permeability retention; FA: Folic acid; FACS: Fluorescence activated cell sorting; FBS: Fetal bovine serum; FDA: Food and Drug Administration; FITC: Fluorescein isothiocyanate; GAPDH: Glyceraldehyde 3-phosphate dehydrogenase; IC50: Half-maximal inhibitory concentration; ICP-OES: Inductively coupled plasma optical emission spectrometry; MRI: Magnetic resonance imaging; MTT: 3-(4,5-Dimethylthiazol-2-yl)-2,5-diphenyltetrazolium bromide; NMR: Nuclear magnetic resonance; NPs: Nanoparticles; PBS: Phosphate buffer saline; PCL: Poly-ε-caprolactone; PE: Plating efficiency; PEG: Poly-ethylene glycol; PI: Propidium iodide; qRT-PCR: Quantitative real time polymerase chain reaction; ROS: Reactive oxygen species; rpm: Revolution per minute; Sn $(Oct)_2$: Stannous octoate; SPION: Superparamagnetic iron oxide nanoparticles; TEM: Transmission electron microscope.

Acknowledgements

Not applicable.

Author contributions

SK and SK were responsible of conception and design of study. PM and SS were responsible of laboratory data acquisition and data analysis. SK as the first author and PM were responsible of article drafting and critical revision. All authors approved the final version of the manuscript.

Funding

This research was funded by Iran University of Medical Sciences (IUMS) (Grant No. 13891). The funders had no role in study design, data collection and analysis, decision to publish, or preparation of the manuscript.

Availability of data and materials

All data generated or analyzed during this study are included in this published article.

Declarations

Ethics approval and consent to participate

Not applicable.

Consent for publication
Not applicable.

Competing interests
The authors declare that they have no competing interests.

Author details
[1]Finetech in Medicine Research Center, Iran University of Medical Sciences, P.O. Box: 1449614525, Tehran, Iran. [2]Department of Medical Physics, School of Medicine, Iran University of Medical Sciences, P.O. Box: 1449614525, Tehran, Iran. [3]Department of Polymer Chemistry, School of Chemistry, College of Science, University of Tehran, Tehran, Iran.

Received: 2 December 2021 Accepted: 25 April 2022
Published online: 16 May 2022

References

Afzalipour R et al (2019) Dual-targeting temozolomide loaded in folate-conjugated magnetic triblock copolymer nanoparticles to improve the therapeutic efficiency of rat brain gliomas. ACS Biomater Sci Eng 5(11):6000–6011
Akinyelu J, Singh M (2019) Folate-tagged chitosan-functionalized gold nanoparticles for enhanced delivery of 5-fluorouracil to cancer cells. Appl Nanosci 9(1):7–17
Almeida BC, Figueiredo P, Carvalho AT (2019) Polycaprolactone enzymatic hydrolysis: a mechanistic study. ACS Omega 4(4):6769–6774
Asadi N et al (2018) Synthesis, characterization and in vitro evaluation of magnetic nanoparticles modified with PCL–PEG–PCL for controlled delivery of 5FU. Artif Cells Nanomed Biotechnol 46(sup1):938–945
Asadi L et al (2018) Cytotoxic effect of 5-fluorouracil-loaded polymer-coated magnetite nanographene oxide combined with radiofrequency. Anti-Cancer Agents Med Chem Formerly Curr Med Chem Anti-Cancer Agents 18(8):1148–1155
Ashour AE et al (2019) Physical pegylation enhances the cytotoxicity of 5-fluorouracil-loaded PLGA and PCL nanoparticles. Int J Nanomed 14:9259
Bodratti AM, Alexandridis P (2018) Amphiphilic block copolymers in drug delivery: advances in formulation structure and performance. Expert Opin Drug Deliv 15(11):1085–1104
Das M, Sahoo SK (2012) Folate decorated dual drug loaded nanoparticle: role of curcumin in enhancing therapeutic potential of nutlin-3a by reversing multidrug resistance. PLoS ONE 7(3):e32920
de Mattos AC et al (2016) Polymeric nanoparticles for oral delivery of 5-fluorouracil: Formulation optimization, cytotoxicity assay and pre-clinical pharmacokinetics study. Eur J Pharm Sci 84:83–91
Didion CA, Henne WA (2020) A Bibliometric analysis of folate receptor research. BMC Cancer 20(1):1–9
Esmaelbeygi E et al (2015) Role of iron oxide core of polymeric nanoparticles in the thermosensitivity of colon cancer cell line HT-29. Int J Hyperth 31(5):489–497
Eynali S et al (2017) Evaluation of the cytotoxic effects of hyperthermia and 5-fluorouracil-loaded magnetic nanoparticles on human colon cancer cell line HT-29. Int J Hyperth 33(3):327–335
Ferrari R et al (2013) Synthesis of surfactant free PCL–PEG brushed nanoparticles with tunable degradation kinetics. Int J Pharm 453(2):551–559
Handali S et al (2018) A novel 5-Fluorouracil targeted delivery to colon cancer using folic acid conjugated liposomes. Biomed Pharmacother 108:1259–1273
Handali S et al (2019) Co-delivery of 5-fluorouracil and oxaliplatin in novel poly (3-hydroxybutyrate-*co*-3-hydroxyvalerate acid)/poly (lactic-*co*-glycolic acid) nanoparticles for colon cancer therapy. Int J Biol Macromol 124:1299–1311
Khoei S et al (2021) Enhancement of radio-thermo-sensitivity of 5-iodo-2-deoxyuridine-loaded polymeric-coated magnetic nanoparticles triggers apoptosis in U87MG human glioblastoma cancer cell line. Cell Mol Bioeng 14:1–13
Kumari S, Kondapi AK (2017) Lactoferrin nanoparticle mediated targeted delivery of 5-fluorouracil for enhanced therapeutic efficacy. Int J Biol Macromol 95:232–237
Lin WJ, Wang CL, Juang LW (2006) Characterization and comparison of diblock and triblock amphiphilic copolymers of poly (δ-valerolactone). J Appl Polym Sci 100(3):1836–1841
Longley DB, Harkin DP, Johnston PG (2003) 5-fluorouracil: mechanisms of action and clinical strategies. Nat Rev Cancer 3(5):330–338
Lu Y et al (2018) Micelles with ultralow critical micelle concentration as carriers for drug delivery. Nat Biomed Eng 2(5):318–325
Mirzaghavami PS et al (2021) Radio-sensitivity enhancement in HT29 cells through magnetic hyperthermia in combination with targeted nano-carrier of 5-Flourouracil. Mater Sci Eng, C 124:112043
Mohammadi Gazestani A et al (2018) In vivo evaluation of the combination effect of near-infrared laser and 5-fluorouracil-loaded PLGA-coated magnetite nanographene oxide. Artif Cells Nanomed Biotechnol 46(sup2):25–33
Nguyen THA, Nguyen VC (2010) Formation of nanoparticles in aqueous solution from poly (ε-caprolactone)–poly (ethylene glycol)–poly (ε-caprolactone). Adv Nat Sci Nanosci Nanotechnol 1(2):025012
Oghabian M et al (2011) Detectability of Her2 positive tumors using monoclonal antibody conjugated iron oxide nanoparticles in MRI. J Nanosci Nanotechnol 11(6):5340–5344
Piasentin N, Milotti E, Chignola R (2020) The control of acidity in tumor cells: a biophysical model. Sci Rep 10(1):13613
Plasencia C et al (2006) Expression analysis of genes involved in oxaliplatin response and development of oxaliplatin-resistant HT29 colon cancer cells. Int J Oncol 29(1):225–235
Qiu L, Dong C, Kan X (2018) Lymphoma-targeted treatment using a folic acid-decorated vincristine-loaded drug delivery system. Drug Des Dev Ther 12:863

Rajpoot K, Jain SK (2020) Oral delivery of pH-responsive alginate microbeads incorporating folic acid-grafted solid lipid nanoparticles exhibits enhanced targeting effect against colorectal cancer: a dual-targeted approach. Int J Biol Macromol 151:830–844
Sharma A et al (2017) Stealth recombinant human serum albumin nanoparticles conjugating 5-fluorouracil augmented drug delivery and cytotoxicity in human colon cancer, HT-29 cells. Colloids Surf B 155:200–208
Shirvalilou S et al (2020) Enhancement radiation-induced apoptosis in C6 glioma tumor-bearing rats via pH-responsive magnetic graphene oxide nanocarrier. J Photochem Photobiol, B 205:111827
Siegel RL et al (2017) Colorectal cancer statistics, 2017. CA Cancer J Clin 67(3):177–193
Song Y et al (2012) Fluorescent carbon nanodots conjugated with folic acid for distinguishing folate-receptor-positive cancer cells from normal cells. J Mater Chem 22(25):12568–12573
Stylianopoulos T (2013) EPR-effect: utilizing size-dependent nanoparticle delivery to solid tumors. Ther Deliv 4(4):421–423
Wang S et al (2001) Degradation and 5-fluorouracil release behavior in vitro of polycaprolactone/poly (ethylene oxide)/polylactide tri-component copolymer† 1. Polym Adv Technol 12(3–4):253–258
Wang Y et al (2012) Pharmacokinetics and disposition of nanomedicine using biodegradable PEG/PCL polymers as drug carriers. Curr Drug Metab 13(4):338–353
Wang Y et al (2015) Targeted delivery of 5-fluorouracil to HT-29 cells using high efficient folic acid-conjugated nanoparticles. Drug Deliv 22(2):191–198
Wang Q et al (2016) Targeted delivery of low-dose dexamethasone using PCL–PEG micelles for effective treatment of rheumatoid arthritis. J Control Release 230:64–72
Wang H et al (2017) A facile strategy for fabricating PCL/PEG block copolymer with excellent enzymatic degradation. Polym Degrad Stab 140:64–73
Zamani S, Khoee S (2012) Preparation of core–shell chitosan/PCL-PEG triblock copolymer nanoparticles with ABA and BAB morphologies: Effect of intraparticle interactions on physicochemical properties. Polymer 53(25):5723–5736
Zhao X, Li H, Lee RJ (2008) Targeted drug delivery via folate receptors. Expert Opin Drug Deliv 5(3):309–319
Zhou M et al (2019) Overcoming chemotherapy resistance via simultaneous drug-efflux circumvention and mitochondrial targeting. Acta Pharmaceut Sin B 9(3):615–625

Publisher's Note